Journal of Electroanalytical Chemistry 847 (2019) 113260

Contents lists available at ScienceDirect

Journal of Electroanalytical Chemistry

journal homepage: www.elsevier.com/locate/jelechem

Tuning molecular energy levels and band gap of two-dimensional benzo[1,2-*b*:4,5-*b′*] dithiophene and quinoxaline bearing polymers

Mustafa Yasa[a], Seza Goker[b], Yasemin Arslan Udum[c], Levent Toppare[a,b,d,e,*]

[a] Department of Polymer Science and Technology, Middle East Technical University, 06800 Ankara, Turkey
[b] Department of Chemistry, Middle East Technical University, 06800 Ankara, Turkey
[c] Ataturk Vocational School, Gazi University, 06374 Ankara, Turkey
[d] Center for Solar Energy Research and Applications, Middle East Technical University, 06800 Ankara, Turkey
[e] Department of Biotechnology, Middle East Technical University, 06800 Ankara, Turkey

ARTICLE INFO

Keywords:
Quinoxaline
Furan
Selenophene
Benzodithiophene
Stille polycondensation
Organic solar cells (OSCs)

ABSTRACT

Two novel donor-acceptor (D-A)-type two-dimensional (2-D) polymers of PBDTSeQ (P1) and PBDTFQ (P2) were synthesized and characterized where 4,8-bis[5-(2-ethylhexyl) thiophen-2-yl] benzo[1,2-b:4,5-b'] dithiophene (BDT) was used as the donor unit. 2,3-Bis(3,4-bis(octyloxy)phenyl)-5,8-dibromoquinoxaline was used as the acceptor moiety and selenophene and furan were utilized as π bridges. Optoelectronic properties of the polymers were examined by electrochemical and spectroelectrochemical characterizations. In cyclic voltammetry (CV) studies, both polymers were found to be ambipolar. In anodic region, oxidation potentials were observed as 1.45 V and 1.15 V for P1 and P2 respectively, while reduction potentials were 0.65 V and 0.92 V. In cathodic region, redox potentials were found to be −1.36 V/−1.32 V and −2.0 V/−1.51 V for P1 and −1.45 V/−1.05 V and −2.15 V/−1.45 V for P2. Both polymers showed good solubility in common solvents. The synthesized polymers were used as photoactive layers in solar cell devices. P1-based device (ITO/PEDOT:PSS/P1:$PC_{71}BM$ (1:3, w/w)/LiF/Al) provided the best performance with a PCE of 4.04%, a V_{OC} of 0.67 V, a J_{SC} of 13.94 mA/cm^2, and a FF of 43.3%.

1. Introduction

Quinoxaline (Qx) and its derivatives are promising materials due to their flat and rigid conjugated structures, and their easy structural modification by attaching various side chains which allows to finely tune their optical properties. Quinoxaline based polymers are widely employed in many fields of applications such as organic solar cells (OSCs), dyes or as ligands in luminescent materials or for metal complication in catalysis [1–3]. The syntheses of quinoxaline monomers or polymers are quite straight forward and usually result in high yields. In addition, quinoxaline monomers and intermediate compounds with relatively short and linear alkyl chain groups can be purified by recrystallization from appropriate solvents without further purifications [4,5]. Due to its easy production, quinoxaline was combined with various donor units like fluorene indacenodithiophene (IDT) [6], thiophene [7], benzodithiophene (BDT) [8,9], dithienosilole (DTS) [10]. Furthermore, quinoxaline derivatives are generally highly stable under ambient conditions due to their low lying highest occupied molecular orbital (HOMO) level which makes them a suitable material for large scale production [11]. To tune optoelectronic properties of conjugated polymers, one approach is to vary the heterocycle by replacing thiophene with selenophene. Selenium is larger and more polarizable which improve intermolecular contacts in polymer thin films, resulting in improved charge carrier mobility in some cases. In addition, lower aromaticity of selenophene in comparison to thiophene also results in improved delocalization of the conjugated system with a reduced optical band gap. These desirable properties have prompted much interest in selenophene containing polymers for both organic solar cell and transistor applications [12]. In literature, there are several examples for selenophene containing conjugated polymers which have been reported with improved device performance, especially charge carrier mobility, over their thiophene-containing analogues [13–17].

Yet, Frechet and co-workers reported that conjugated polymers comprising of furan moieties have enhanced solubility in common organic solvents even with the use of relatively small solubilizing side chains compared to thiophene containing counterparts. The mechanism behind the improved solubility imparted by the furan co-monomer is not well established, however atomic radius and electronegativity

* Corresponding author at: Department of Biotechnology, Middle East Technical University, 06800 Ankara, Turkey.
E-mail address: toppare@metu.edu.tr (L. Toppare).

https://doi.org/10.1016/j.jelechem.2019.113260
Received 26 April 2019; Received in revised form 17 June 2019; Accepted 22 June 2019
Available online 26 June 2019
1572-6657/ © 2019 Elsevier B.V. All rights reserved.

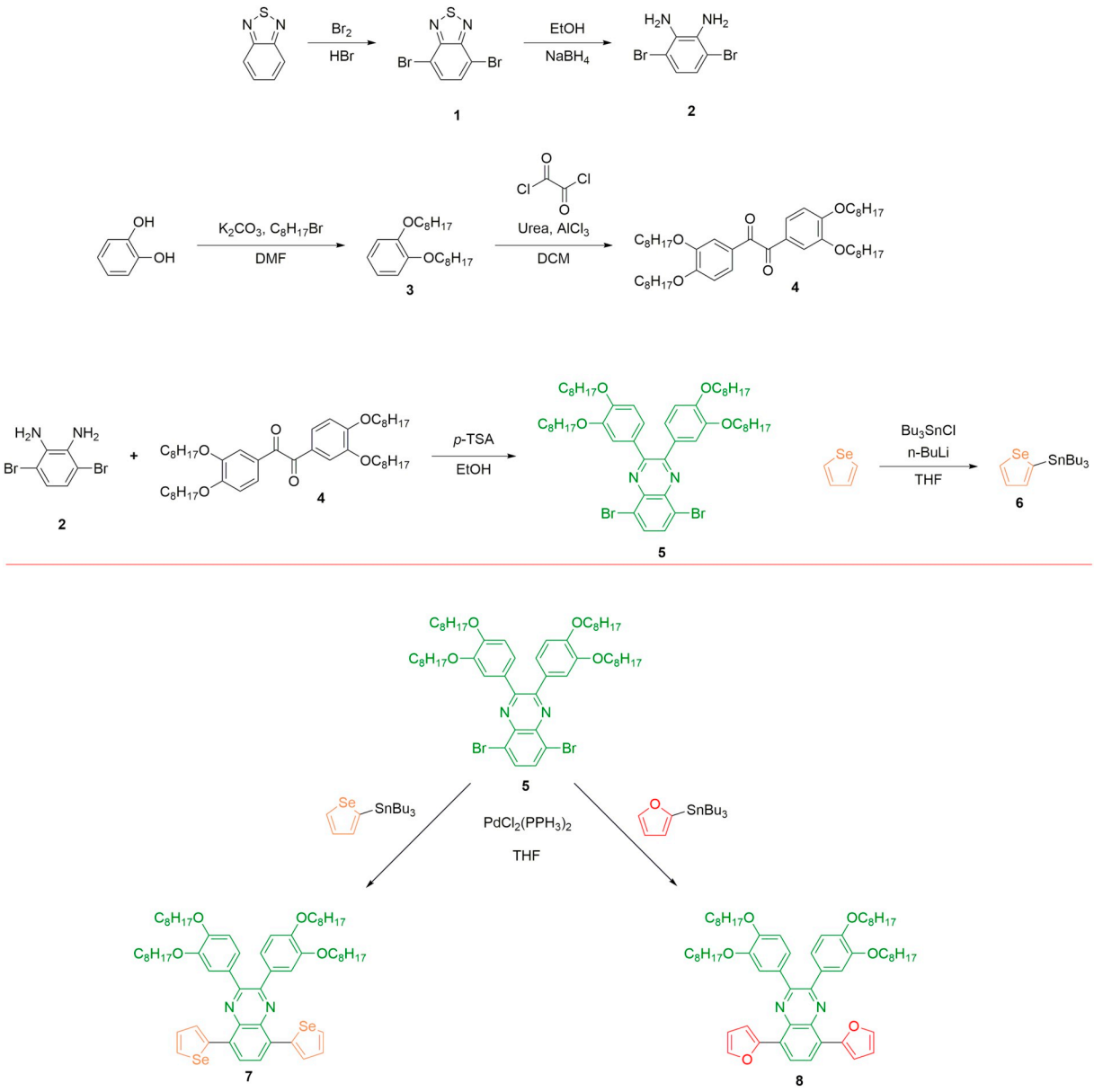

Scheme 1. Synthetic pathway for monomers

differences between oxygen and sulfur atoms might affect solvent interactions, intermolecular interactions, and intramolecular steric interactions which could result in enhanced solubility [18–20]. It has been shown that higher molecular weight polymers can be obtained with the substitution of furan for thiophene in the main chain of the polymer due to enhanced solubility. The formation of high-quality films of active layer with highly soluble polymers provides efficient charge generation and collection for OSCs. Besides, Li and co-workers state that incorporation of furan could lower the HOMO energy level, thus increasing the open circuit voltage (V_{oc}) of solar cells [21,22]. In addition, furan-based materials which are biodegradable can be prepared from bio renewable sources making them more suitable for low-cost and large-scale applications. Based on the above results, further investigation for furan-based OSCs is definitely needed [23]. Its structural symmetry and rigid fused aromatic system make benzo[1,2-*b*:4,5-*b*'] dithiophene (BDT) highly popular electron donating moiety since it could enhance electron delocalization and improve charge mobility [24]. To illustrate, thiophene substituted BDT, 5-alkylthiophene-2-yl-substituted benzo[1,2-*b*:4,5-*b*'] dithiophene (BDTT), moieties have been extensively used as donor units over a couple of years. Several copolymers of BDTT with benzothiadiazole (BT) [25,26], diketopyrrolopyrrole (DPP) [27,28], and thieno [3,4-b] thiophene (TT) [21], have shown enhanced thermal stabilities, lower HOMO and LUMO energy levels, higher hole mobility, and improved photovoltaic performance compared to their corresponding alkoxy-substituted BDT derivatives [29]. In 2014, Hou and coworkers synthesized 2D-conjugated BDT based polymers replacing alkoxy-substituted BDT with alkylthienyl-substituted BDT which could improve the polymer hole mobility substantially with little effect on their molecular energy level. It is concluded that introduction of 2-D-conjugated structure results in broader absorption band, lower HOMO level and higher hole mobility, hence better photovoltaic results. PCE of the OSC devices based on the 2D polymers, were 50% and 20% higher than their analogues with one-dimensional conjugated backbone, respectively. 2-D conjugated structure is beneficial to improve photovoltaic properties of the narrow band gap D/A-polymer system without quinoid properties [30]. Inspired by the previous reports, we have designed and synthesized new quinoxaline and benzodithiophene based polymers using furan and selenophene as the π bridges in the polymer backbone. The effect of heterocycle nature on optical and electrochemical properties is investigated in

detail. P1 and P2 were also used in conjunction with phenyl-C_{70}-butyric acid methyl ester ($PC_{71}BM$) in order to construct bulk heterojunction solar cells.

2. Materials and methods

2.1. General

All chemicals and solvents were purchased from Aldrich/Merck. 4,8-Bis[5-(2-ethylhexyl) thiophen-2-yl]-2,6-bis(trimethylstannyl)benzo [1,2-*b*:4,5-*b*'] dithiophene was used without further purification. Phenyl-C_{70}-butyric acid methyl ester ($PC_{71}BM$) was purchased from Ossila. Tetrahydrofuran (THF) and toluene were freshly distilled prior to use. ^1H and ^{13}C NMR spectra were recorded using Bruker Spectrospin Avance DPX-400 Spectrometer. Chemical shifts were reported as δ values (ppm) relative to tetramethylsilane (TMS) where δ (TMS) = 0. Number-average ($\overline{M}_n$) and weight average ($\overline{M}_w$) molecular weights were determined by size exclusion chromatography (SEC) using a high temperature Shimadzu LC-20AT GPC in chloroform at 45 °C calibrated against polystyrene standards. Column chromatography was carried out with Merck Silica Gel 60 (particle size: 0.063–0.200 mm, 70–230 mesh ASTM). Varian Cary 5000 UV–Vis spectrophotometer was used to perform spectroelectrochemical studies. Cyclic voltammetry (CV) of the polymer films was performed using a GAMRY Reference 600 potentiostat at a scan rate of 100 mV/ s; the solvent was acetonitrile (ACN), containing 0.1 M tetrabutylammonium hexafluorophosphate ($TBAPF_6$) as the supporting electrolyte. The onset potentials were determined from the cyclic voltammograms. The synthetic route toward monomer and polymer are shown in Schemes 1 and 2.

2.1.1. Synthesis of 4,7-dibromobenzo[c] [1,2,5] thiadiazole (1)

Benzo[c] [1,2,5] thiadiazole (5.0 g, 37 mmol) was introduced into a three-necked flask charged with a stirring bar. HBr (48%, 90 mL) was added and the solution was heated. At 100 °C, HBr-Br_2 mixture (44 mL) was added drop wise. After addition of HBr/Br_2, the temperature was set to 135 °C and the solution was stirred overnight. The reaction mixture was kept in ice bath for 2 h to settle the product. The precipitate was filtered and washed with $NaHSO_3$ in order to remove possible excess bromine. Then, the crude product was dissolved in dichloromethane (DCM) and the organic layers were washed with water. The organic layers were combined and dried over Na_2SO_4. The solvent was evaporated under reduced pressure. The product was washed with diethyl ether to remove mono brominated benzothiadiazole. Yield: 9.7 g, 90%.

^1H NMR (400 MHz, $CDCl_3$): δ: 7.73 (s, 2H).

^{13}C NMR (100 MHz, $CDCl_3$): δ: 153.0, 132.3, 114.1.

2.1.2. Synthesis of 3,6-dibromobenzene-1,2-diamine (2)

4, 7-Dibromobenzo[c][1,2,5]thiadiazole (1.0 g, 3.4 mmol) was dissolved in ethanol (25 mL) in a 1 L Erlenmeyer charged with a stirring bar. The solution was cooled to 0 °C. $NaBH_4$ (5.0 g, 132 mmol) kept under argon atmosphere was added portion wise to the solution. The mixture was warmed to room temperature and stirred overnight. The solvent was removed under reduced pressure. The crude product was dissolved in diethyl ether. The organic layers were washed with water. The organic layer was dried over anhydrous Na_2SO_4. The evaporation of solvent under reduced pressure afforded the product as a white solid. Yield: 0.75 g, 83%.

^1H NMR (400 MHz, $CDCl_3$): δ: 6.85 (d, 2H), 3.89 (s, 4H).

^{13}C NMR (100 MHz, $CDCl_3$): δ: 133.7, 123.3, 109.7.

2.1.3. Synthesis of 1,2-bis(octyloxy)benzene (3)

Catechol (4.0 g, 36 mmol), K_2CO_3 (13 g, 94 mmol) and 1-bromooctane (14 g, 73 mmol) were put into a two-necked 100 mL flask under argon atmosphere. Anhydrous DMF (35 mL) was added to the flask and the solution was heated to 100 °C. Thin Layer Chromatography (TLC) controlled reaction was stirred overnight. The solvent was removed using rotary evaporator. Then, the crude product was dissolved in dichloromethane. The organic phase was washed with water and brine several times, respectively. Na_2SO_4 was used to dry organic layer. The solvent was removed under reduced pressure and the product was recrystallized from cold methanol. A milky brown solid was obtained. Yield: 9.9 g, 81%.

^1H NMR (400, $CDCl_3$): δ: 6.89 (s, 4H), 3.99 (t, J = 6.65 Hz, 4H), 1.81 (m, J = 6.85 Hz, 4H), 1.47 (m, 4H), 1.28–1.37 (m, 16H), 0.88 (t, J = 6.41 Hz, 6H).

^{13}C NMR (100 MHz, $CDCl_3$): δ: 149.3, 121.0, 114.1, 69.3, 31.8, 29.4, 26.1, 22.7, 14.1.

2.1.4. Synthesis of 1,2-bis(3,4-bis(octyloxy)phenyl) ethane-1,2-dione (4)

1,2-Bis(octyloxy)benzene (1.9 g, 5.5 mmol), urea (0.3 g, 5.2 mmol) and $AlCl_3$ (1.1 g, 8.4 mmol) were dissolved in DCM (15 mL). The solution was cooled to 0 °C. Oxalylchloride (0.3 mL, 3.4 mmol) was added drop wise to the solution. After overnight stirring, the dark purple solution was poured into cold water and organic layer was extracted with dichloromethane. Combined organic phase was washed with $NaHCO_3$ several times, dried over Na_2SO_4 and concentrated by rotary evaporation. The product was recrystallized from cold methanol and obtained as a white solid. Yield: 0.99 g, 50%.

^1H NMR (400, $CDCl_3$): δ: 7.56 (d, J = 2.0 Hz, 2H), 7.43 (dd, J_1 = 1.86 Hz, J_2 = 8.36 Hz, 2H), 6.86 (d, 2H), 4.05 (t, J = 5.25 Hz, 8H), 1.84 (m, 8H), 1.45 (m, 8H), 1.28 (m, 32H), 0.88 (m, 12H).

^{13}C NMR (100 MHz, $CDCl_3$): δ: 193.8, 165.7, 155.0, 149.3, 126.1, 121.0, 114.1, 69.3, 31.8, 29.3, 29.1, 26.1, 22.7, 14.1.

2.1.5. Synthesis of 2,3-bis(3,4-bis(octyloxy)phenyl)-5,8-dibromoquinoxaline (5)

3,6-Dibromobenzene-1,2-diamine (0.22 g, 0.85 mmol) and 1,2-bis (3,4-bis(octyloxy)phenyl) ethane-1,2-dione (0.62 g, 0.85 mmol) were added in a 100 mL, two-necked flask under argon atmosphere. The mixture was dissolved in 10 mL ethanol (10 mL) and *p*-toluene sulfonic acid was added in a catalytic amount. The solution was heated and stirred overnight. Then, the mixture was cooled to 0 °C to collect the precipitate. The product was filtered and washed with ethanol to remove residual starting materials. Yield: 0.57 g, 66%.

^1H NMR (400 MHz, $CDCl_3$): δ: 7.85 (s, 2H), 7.56 (d, J = 1.97 Hz, 2H), 7.43 (dd, J_1 = 2.02 Hz, J_2 = 8.44 Hz, 2H), 6.85 (d, J = 2.11 Hz, 2H), 4.0 (t, J = 6.67 Hz, 8H), 1.74 (m, 8H), 1.47 (m, 8H), 1.29 (m, 32H), 0.89 (m, 12H).

^{13}C NMR (100 MHz, $CDCl_3$): δ: 151.5, 148.6, 146.6, 136.9, 130.4, 128.5, 121.3, 113.5, 110.9, 67.1, 29.7, 27.3, 23.9, 20.6, 12.0.

2.1.6. Synthesis of tributyl(selenophen-2-yl) stannane (6)

Selenophene (5.0 g, 38 mmol) was dissolved in anhydrous tetrahydrofuran (70 mL) in a two-necked, 50 mL flask under inert atmosphere. After the solution was cooled to −78 °C, n-butyl lithium (15 mL, 38 mmol in 2.5 M hexane) was added drop wise to the reaction medium. After addition was completed, the system was maintained at −78 °C for additional 1 h. Tributyltin chloride (11 mL, 41 mmol) was added drop wise. The solution was warmed to room temperature slowly and left to stir overnight. After removing the solvent by rotary evaporation, dichloromethane was poured into the crude product and organic layer was washed with $NaHCO_3$, water and brine. Combined organic layers were dried over anhydrous Na_2SO_4 and concentrated under reduced pressure. The product was obtained as a yellow oil and used without further purification. Yield: 14 g, 95%.

^1H NMR (400 MHz, $CDCl_3$) δ: 8.36 (d, J = 8.36 Hz, 1H), 7.53 (m, 1H), 7.5 (dd, J_1 = 2.44 Hz, J_2 = 9.44 Hz, 1H), 1.59 (m, 6H), 1.37 (m, 6H), 1.12 (m, 6H), 0.91 (t, J = 7.33 Hz, 9H).

^{13}C NMR (100 MHz, $CDCl_3$): δ: 143.6, 137.9, 135.3, 130.6, 29.0, 27.3, 13.6, 11.1.

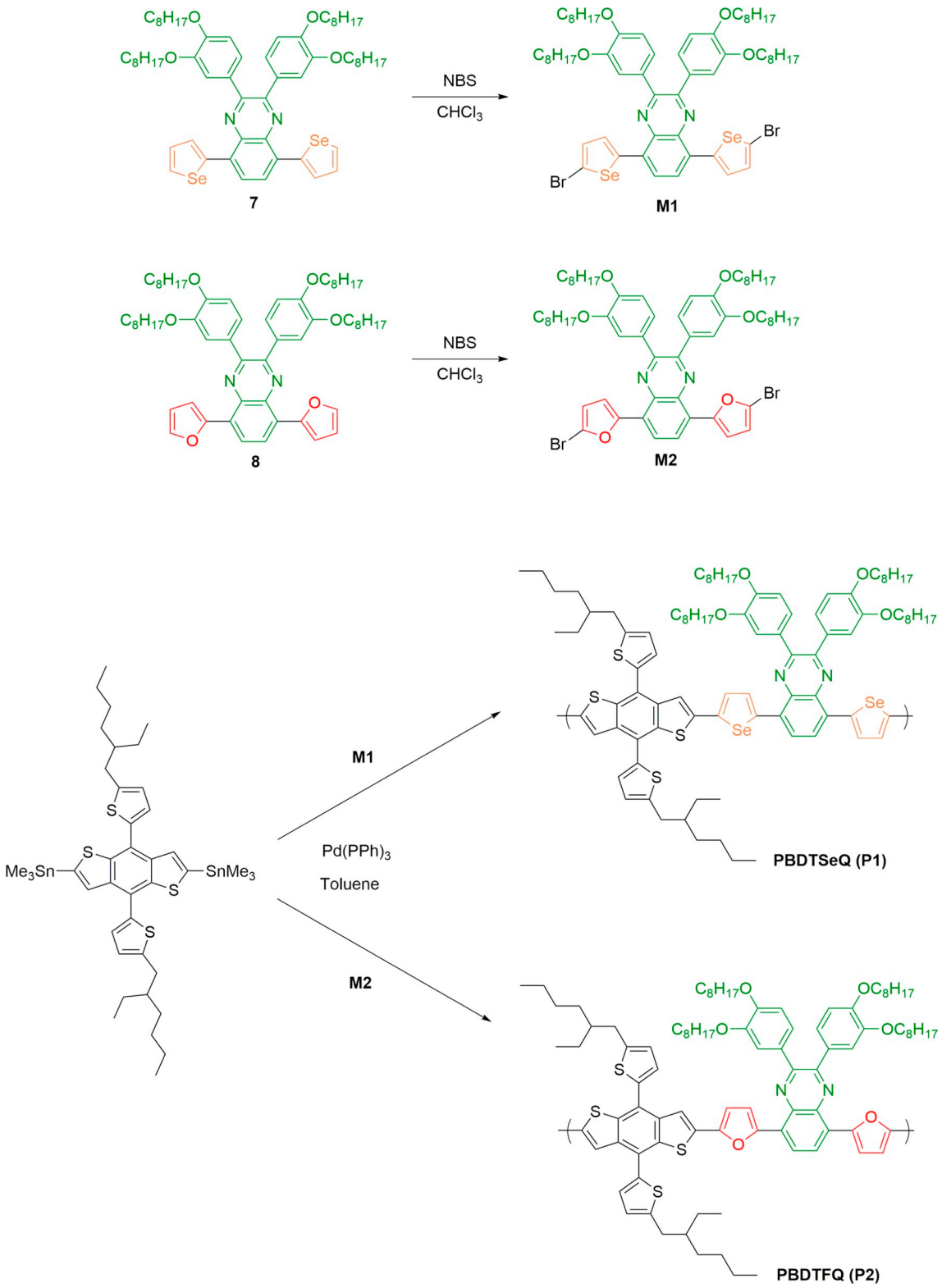

Scheme 2. The syntheses and structures of polymers

2.1.7. Synthesis of 2,3-bis(3,4-bis(octyloxy)phenyl)-5,8-di(selenophen-2-yl)quinoxaline (7)

2,3-Bis(3,4-bis(octyloxy)phenyl)-5,8-dibromoquinoxaline (0.40 g, 0.40 mmol), dry THF (35 mL), $PdCl_2(PPh_3)_2$ (45.0 mg, 16% mmol) and tributyl(selenophen-2-yl) stannane (0.88 mg, 2.10 mmol) were added to a flask under argon atmosphere. The flask was placed in an oil bath and the temperature of the oil bath was set to 100 °C. The solution was stirred for 18 h. Then, the mixture was cooled to room temperature. The evaporation of solvent under reduced pressure afforded a dark red solid which was then purified by column chromatography on silica gel using hexane:chloroform (1:1). Yield: 0.36 g, 95%.

^{1}H NMR (400 MHz, $CDCl_3$) δ: 8.22 (2H, s), 8.19 (d, J = 6.5 Hz, 2H), 8.05 (d, J = 3.2 Hz, 2H), 7.45 (dd, J_1 = 4.0 Hz, J_2 = 5.77 Hz 2H), 7.36 (d, J = 2.0 Hz 2H), 7.23 (dd, J_1 = 2.0 Hz, J_2 = 2.1 Hz, 2H), 6.86 (d,

J = 8.5 Hz, 2H), 4.04 (t, J = 6.65 Hz, 4H), 3.93 (t, J = 6.72 Hz, 4H), 1.86 (m, 4H), 1.78 (m, 4H), 1.40–1.25 (m, 40H), 0.9 (t, J = 6.60 Hz, 12H).

^{13}C NMR (100 MHz, $CDCl_3$): δ: 163.0, 159.2, 151.7, 110.3, 102.4, 85.3, 31.9, 29.4, 26.1, 22.7, 22.2, 14.1.

2.1.8. Synthesis of 2,3-bis(3,4-bis(octyloxy)phenyl)-5,8-di(furan-2-yl) quinoxaline (8)

2,3-Bis(3,4-bis(octyloxy)phenyl)-5,8-dibromoquinoxaline (0.50 g, 0.50 mmol), $PdCl_2(PPh_3)_2$ (20 mg) and tributyl(furan-2-yl) stannane (0.56 g 1.57 mmol) were dissolved in anhydrous THF (44 mL) in a flask placed in an oil bath under inert atmosphere. The oil bath was heated to 100 °C and the mixture was stirred for 18 h. The solution was cooled to room temperature and concentrated under reduced pressure. After evaporation of solvent, a dark red solid was obtained and purified by column chromatography on silica gel using hexane:dichloromethane (1:2). Yield: 0.40 g, 86%.

^{1}H NMR (400 MHz, $CDCl_3$): δ: 8.25 (s, 2H), 7.85 (d, J = 3.2 Hz, 2H), 7.58 (d, J = 1.2 Hz, 2H), 7.24 (d, J = 1.5 Hz, 2H), 7.22 (d, J = 2.0 Hz, 2H), 6.88 (d, J = 8.9 Hz, 2H), 6.6 (dd, J_1 = 3.3 Hz, J_2 = 1.8 Hz, 2H), 4.03 (t, J = 6.7 Hz, 4H), 3.88 (t, J = 6.7 Hz, 4H), 1.85 (p, J = 6.8 Hz, 4H), 1.76 (p, J = 6.7 Hz, 4H), 1.36–1.29 (m, 40H), 0.9 (m, 12H).

^{13}C NMR (100 MHz, $CDCl_3$): δ: 151.4, 150.9, 150.0, 148.6, 142.0, 136.8, 131.9, 127.0, 125.3, 123.0, 115.6, 113.2, 112.3, 69.2, 31.9, 29.4, 26.1, 22.7, 14.1.

2.1.9. Synthesis of 2,3-bis(3,4-bis(octyloxy)phenyl)-5,8-bis(5-bromoselenophen-2-yl) quinoxaline (M1)

2,3-Bis(3,4-bis(octyloxy)phenyl)-5,8 di(selenophen-2-yl) quinoxaline (0.46 g, 0.43 mmol) was dissolved in $CHCl_3$ (8 mL) in a 100 mL flask charged with a stirring bar. N-bromosuccinimide (NBS) (0.15 g, 0.86 mmol) was added to the solution in several portions. The mixture was stirred overnight at ambient temperature. The organic phase was washed with distilled water, dried over Na_2SO_4 and concentrated under reduced pressure. The product was recrystallized from ethanol and obtained as a red solid. Yield: 0.46 g, 89%.

^{1}H NMR (400 MHz, $CDCl_3$) δ: 8.15 (s, 2H), 7.73 (d, J = 4.4 Hz, 2H), 7.41 (s, 2H), 7.36 (d, J = 4.35 Hz, 2H), 7.07 (dd, J_1 = 2.03 Hz, J_2 = 8.32 Hz, 2H), 6.83 (d, J = 8.4 Hz, 2H), 4.03 (t, 8H), 1.85 (m, 8H), 1.50 (m, 8H), 1.25–1.36 (m, 32H), 0.9 (t, J = 6.71 Hz, 12H).

^{13}C NMR (100 MHz, $CDCl_3$): δ: 150.1, 148.1, 146.7, 140.4, 133.6, 129.7, 129.26, 128.3, 123.6, 121.4, 120.8, 113.8, 110.3, 67.3, 29.7, 27.2, 24.0, 20.5, 11.9.

2.1.10. Synthesis of 2,3-bis(3,4-bis(octyloxy)phenyl)-5,8-bis(5-bromofuran-2-yl) quinoxaline (M2)

2,3-Bis(3,4-bis(octyloxy)phenyl)-5,8 di(furan-2-yl) quinoxaline (0.40 g, 0.42 mmol) was dissolved in $CHCl_3$ (10 mL) in a 50 mL flask charged with a stirring bar. N-bromosuccinimide (NBS) (0.15 g, 0.85 mmol) was added to the solution in several portions. The mixture was stirred overnight at ambient temperature. The organic phase was washed with distilled water, dried over Na_2SO_4 and concentrated under reduced pressure. The product was recrystallized from ethanol and obtained as a red solid. Yield: 0.17 g, 36%.

^{1}H NMR (400 MHz, $CDCl_3$): δ: 8.18 (s, 2H), 7.77 (d, J = 3.4 Hz, 2H), 7.20 (d, J = 1.9 Hz, 2H), 7.17 (d, J = 3.3 Hz, 2H), 6.88 (d, J = 8.2 Hz, 2H), 6.49 (d, J = 3.4 Hz, 2H), 4.03 (t, J = 6.7 Hz, 4H), 3.85 (t, J = 6.7 Hz, 4H), 1.85 (p, 4H), 1.74 (m, 4H), 1.37–1.26 (m, 40H), 0.9 (m, 12H).

^{13}C NMR could not be recorded due to instability of monomer.

2.2. Polymer syntheses

2.2.1. Synthesis of PBDTSeQ (P1)

In a two-necked flask under argon atmosphere, 2,3-bis (3,4-bis(octyloxy)phenyl)-5,8-bis(5-bromoselenophen-2-yl) quinoxaline (0.13 g, 0.11 mmol), 4,8-bis[5-(2-ethylhexyl) thiophen-2-yl]-2,6-bis(trimethylstannyl)benzo[1,2-*b*:4,5-*b*'] dithiophene (0.10 g, 0.11 mmol) and $Pd(PPh_3)_4$ (5 mol%) were dissolved in 11 mL dry toluene. The mixture was stirred at 95 °C for 21 h. Chlorobenzene and tributyl(furan-2-yl) stannane were added as end capping reagents and the solution was stirred for additional 7 h. The solvent was removed using rotary evaporator. After addition of methanol, sodium diethyldithiocarbamate trihydrate (10 mg) was added as a palladium scavenger and the solution was stirred for 1 h. After filtration, the crude product was washed with acetone and hexane using Soxhlet extractor to remove low molecular weight fractions. Chloroform was used to collect the polymer. Solvent was removed using rotary evaporator and the polymer was recrystallized from cold methanol to afford dark blue crystals. Yield: 0.16 g, 89%.

^{1}H NMR ($CDCl_3$, 400 MHz): δ: 7.69, 7.52 (Phenyl), 7.34, 6.95 (Quinoxaline), 7.20 (Selenophene), 6.84 (Thiophene), 4.05, 3.86 (-OCH_2), 1.89, 1.71 (-Ethyl Hexyl), 1.33, 1.25, 1.11 (-CH_2), 0.91, 0.78 (-CH_3).

M_n: 16000 Da, M_w: 22000 Da, PDI: 1.37.

2.2.2. Synthesis of PBDTFQ (P2)

Similar polymerization procedure was used for the preparation of PBDTFQ. 2,3-Bis(3,4-bis(octyloxy)phenyl)-5,8-bis(5-bromofuran-2-yl) quinoxaline (0.14 g, 0.13 mmol), 4,8-bis[5-(2-ethylhexyl) thiophen-2-yl]-2,6-bis(trimethylstannyl)benzo[1,2-b:4,5-b'] dithiophene (0.12 g, 0.13 mmol) and $Pd(PPh_3)_4$ (5 mol%) were dissolved in anhydrous toluene (10 mL) and polymerized to give PBDTFQ. Yield: 0.15 g, 75%.

^{1}H NMR ($CDCl_3$, 400 MHz): δ: 8.24, 8.22, 8.20 (Quinoxaline), 8.12, 8.08 (Phenyl), 7.73, 7.68, 7.64, 7.62, 7.60 (Phenyl), 7.43 (Fused Thiophene), 7.34, 7.33 (Thiophene), 6.91, 6.90, 6.89 (Furan), 4.22, 4.06, 3.96, 3.90 (-OCH_2), 2.04, 1.88, 1.75, 1.68 (-Ethyl Hexyl), 1.38, 1.32, 1.25, 1.24, 1.6, 1.19 (-CH_2), 0.91, 0.89, 0.84, 0.79, 0.78 (-CH_3).

M_n: 6020 Da, M_w: 8020 Da, PDI: 1.33.

2.3. Device fabrication

ITO coated glass substrates (15 Ohm/sq) were purchased from Visiontek Systems. ITO electrodes were cleaned with detergent water, water and isopropyl alcohol in ultrasonic bath. Substrates were dried with N_2 gun and exposed to oxygen plasma cleaning. PEDOT:PSS was spin coated in ambient conditions. Active layer blends were dissolved in 1,2-dichloro benzene (*o*-dcb) and spin coated in glove box. 0.6 nm LiF and 100 nm Al were evaporated onto the active layer. Resulting device structure is ITO/PEDOT:PSS/Polymer:$PC_{71}BM$/LiF:Al. *J-V* characterizations were carried out under AM 1.5 G solar simulator in glove box.

3. Results

3.1. Electrochemical and optical properties

Reduction and oxidation behaviors of the polymers and their HOMO and LUMO levels were determined by cyclic voltammetry (CV). Upon dissolving 3 mg of each polymer in 1 mL of chloroform, the solution was spray coated on ITO coated glass substrate. Single scan cyclic voltammograms of the polymers were obtained at ambient temperature in a three electrode system in a solution of 0.1 M tetrabutylammonium hexafluorophosphate in acetonitrile ($TBAPF_6$/ACN). ITO was employed as the working electrode while a platinum and a silver wire were used as counter and reference electrodes, respectively. The voltammograms of the polymers were obtained by cycling at a scan rate of 100 mV/s (Figs. 1).

CV studies showed that P1 and P2 are ambipolar, showing both p-dopable and n-dopable characteristics. In anodic region, oxidation potential for P1 was determined as 1.45 V while the reduction potential was 0.65 V. During the potential application in the cathodic region, two

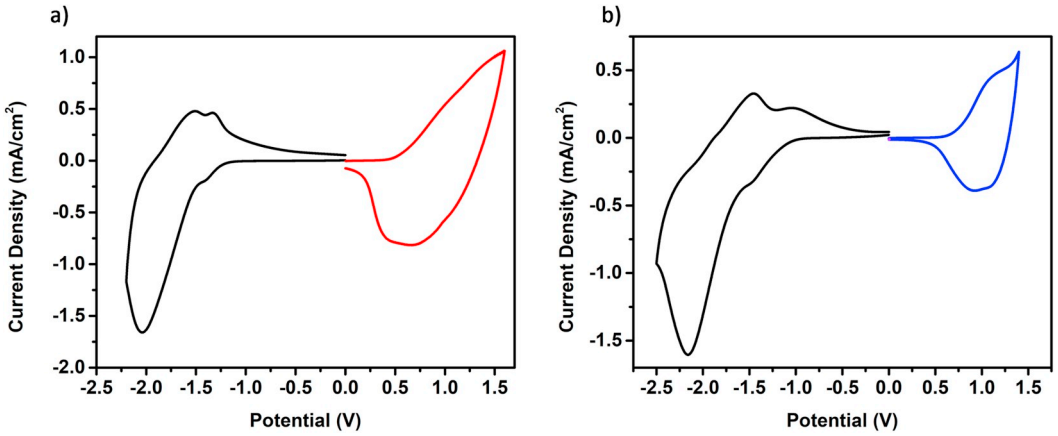

Fig. 1. Single scan cyclic voltammograms of polymers (a) P1, (b) P2 on ITO in 0.1 M $TBAPF_6$/ACN electrolyte/solvent couple at a scan rate of 100 $mV{\cdot}s^{-1}$.

Table 1
Comparison of electronic properties of P1 and P2.

	$E_{p\text{-doping}}$ (V)	$E_{p\text{-dedoping}}$ (V)	$E_{n\text{-doping}}$ (V)	$E_{n\text{-dedoping}}$ (V)	HOMO (eV)	LUMO (eV)	E_g^{ec} (eV)	E_g^{op} (eV)
P1	1.45	0.65	−1.36/−2.0	−1.32/−1.51	−5.24	−3.57	1.67	1.65
P2	1.15	0.92	−1.45/−2.15	−1.05/−1.45	−5.47	−3.68	1.79	1.40

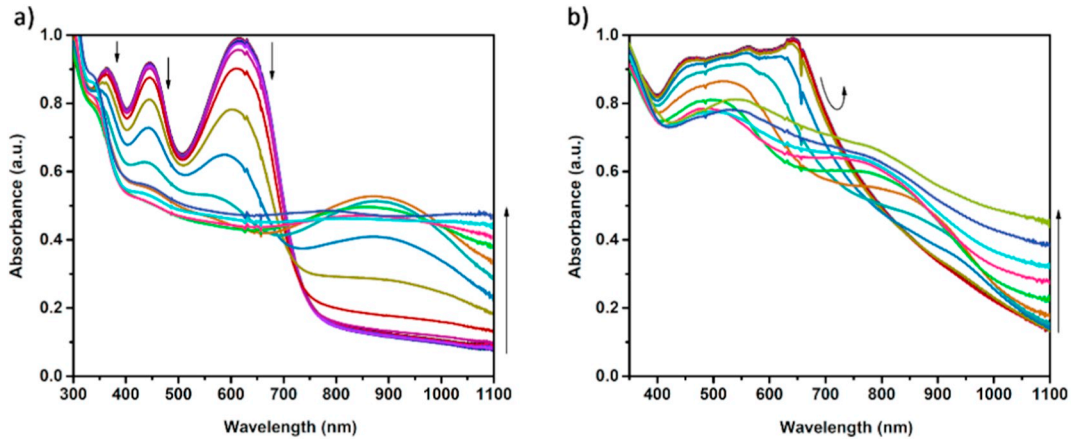

Fig. 2. Electronic absorption spectra for (a) P1 and (b) P2 in 0.1 M $TBAPF_6$/ACN solution.

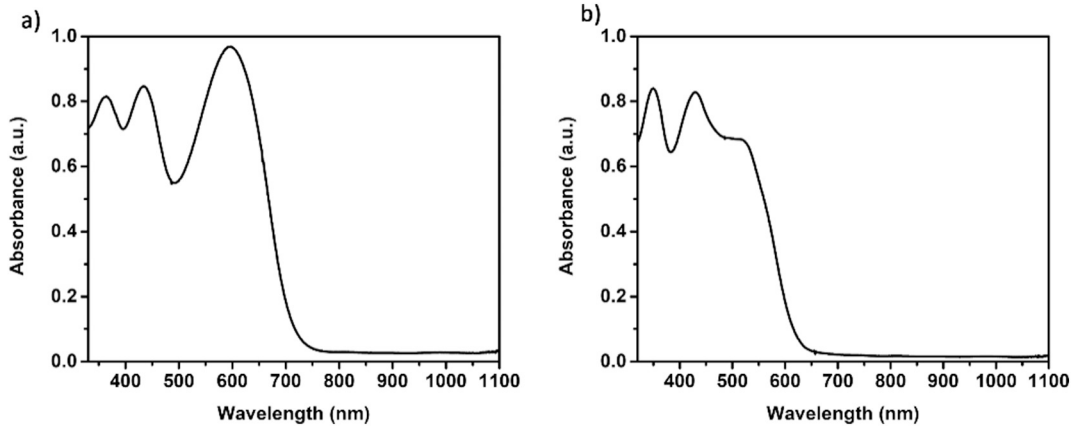

Fig. 3. Electronic absorption spectra for (a) P1 and (b) P2 in 0.1 M $TBAPF_6$/ACN solution.

redox peaks were observed. The redox couples were observed at −1.36 V/−1.32 V, and at −2.00 V/−1.51 V, respectively. Oxidation and reduction potentials for P2 were determined as 1.15 V and 0.92 V, respectively and redox couples were observed at −1.45 V/−1.05 V and −2.15 V/−1.45 V, respectively.

HOMO and LUMO levels of polymers were determined with respect

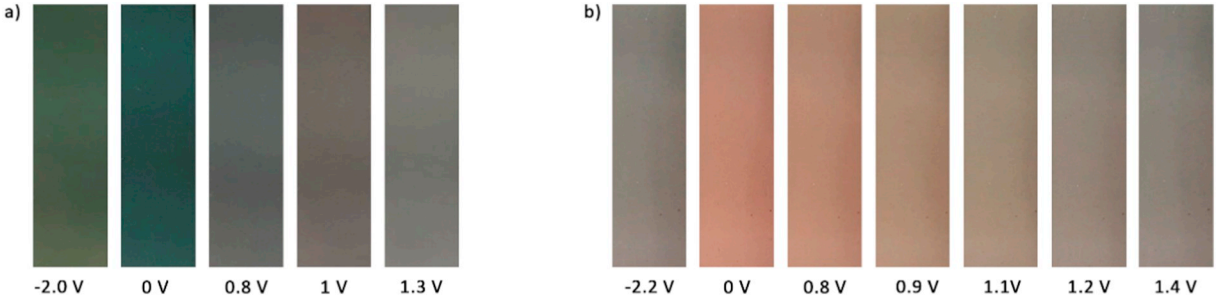

Fig. 4. Colors of (a) P1 and (b) P2.

Table 2
Colorimetry measurements of P1 and P2.

	Applied potential (V)	L	a	b
P1	−2.0	30.58	−8.647	8.219
	0	21.44	−8.562	−1.991
	0.8	35.19	−3.218	1.734
	1.0	37.39	0.555	5.844
	1.3	40.47	−1.312	5.055
P2	−2.2	44.97	3.625	3.344
	0	53.46	15.09	17.64
	0.8	54.13	11.45	17.30
	0.9	52.18	6.977	15.61
	1.1	53.15	2.688	11.92
	1.2	49.61	1.664	8.469
	1.4	47.76	0.938	6.289

Table 3
Optical transmittance changes and switching times of P1 and P2.

	Wavelength (nm)	Transmittance (%)	Switching time (s)
P1	445	20	1.2
	615	30	2.0
P2	645	11	1.3

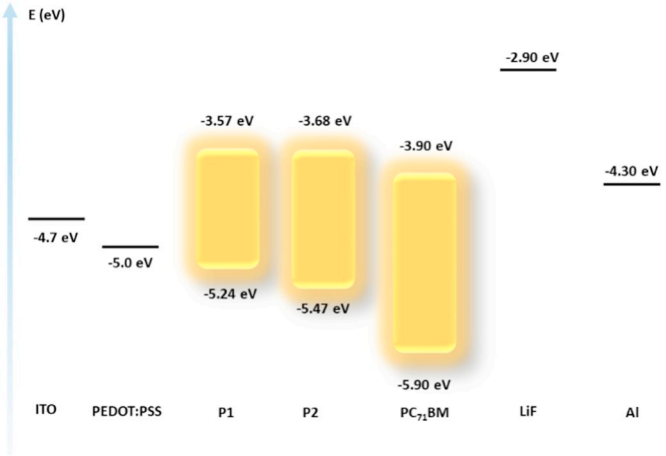

Fig. 5. Energy level diagram of the OSCs based on P1 and P2.

Table 4
Photovoltaic characteristics of P1:$PC_{71}BM$-based OSCs.

Polymer:$PC_{71}BM$	V_{OC} (V)	J_{SC} (mA/cm^2)	FF (%)	PCE (%)
P1:$PC_{71}BM$ (1:1, w:w)	0.67	8.44	39.4	2.22
P1:$PC_{71}BM$ (1:2, w:w)	0.69	8.21	43.0	2.43
P1:$PC_{71}BM$ (1:3, w:w)	0.67	13.94	43.3	4.04
P1:$PC_{71}BM$ (1:4, w:w)	0.73	6.94	51.3	2.60
P1:$PC_{71}BM$ (1:3, w:w) (3% DPE)	0.69	8.53	48.0	2.82

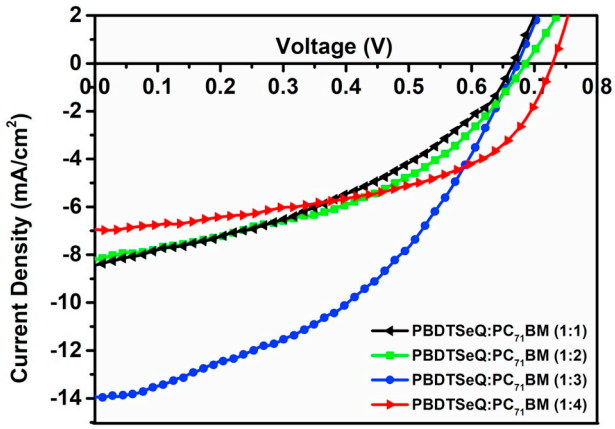

Fig. 6. *J-V* curves of P1:$PC_{71}BM$-based OSCs with different Polymer:$PC_{71}BM$ ratios.

to normal hydrogen electrode (NHE), −4.75 eV against vacuum using oxidation onset and reduction onset potentials, respectively. Onset potentials were obtained from an intersection of the baseline and the tangent to the redox peaks. The following formulae provide energy levels versus vacuum.

$$E_{HOMO} = -(E_{onset,ox} + 4.75)\ (\text{eV})$$

$$E_{LUMO} = -(E_{onset,red} + 4.75)\ (\text{eV})$$

Electronic band gaps of the polymers were determined from the following equation;

$$E_g^{ec} = HOMO - LUMO\ (\text{eV})$$

Electrochemical properties of the polymers are represented in Table 1.

For the investigation of the optical and electronic changes of the polymer spectroelectrochemical tests were performed. To carry out the spectroelectrochemical studies, 3 mg polymer were dissolved in 1 mL of chloroform, and the solution was spray coated on a glass substrate coated with indium tin oxide (ITO). Obtained films were placed in a cell containing a solution of 0.1 M tetrabutylammonium hexafluorophosphate in acetonitrile ($TBAPF_6$/ACN), electrolyte/solvent system. The polymer film was doped stepwise via the applied potential.

Absorption changes were recorded as a function of wavelength. A potential range between 0 V and 1.2 V was applied.(Fig. 2) π-π* corresponding λ_{max} values for P1 and P2 were determined as 445 nm/615 nm and 645 nm, respectively. The onset absorption values of P1 and P2, λ_{onset}, were 752 nm and 885 nm, respectively. (Fig. 3)

P1 film showed grayish color under 0.8 V, grayish pink under 1.0 V, and light gray under 1.5 V potential at oxidation state whereas became greenish under −0.5 V potential at reduction state. P2 film is pink/gray at 1.1 V and gray at 1.4 V. (Fig. 4) The optical band gap values of the polymers were calculated from the equation $E_g^{op} = 1241/\lambda_{onset}$. Inserting the λ_{onset} value into the equation, the band gap for P1 and P2

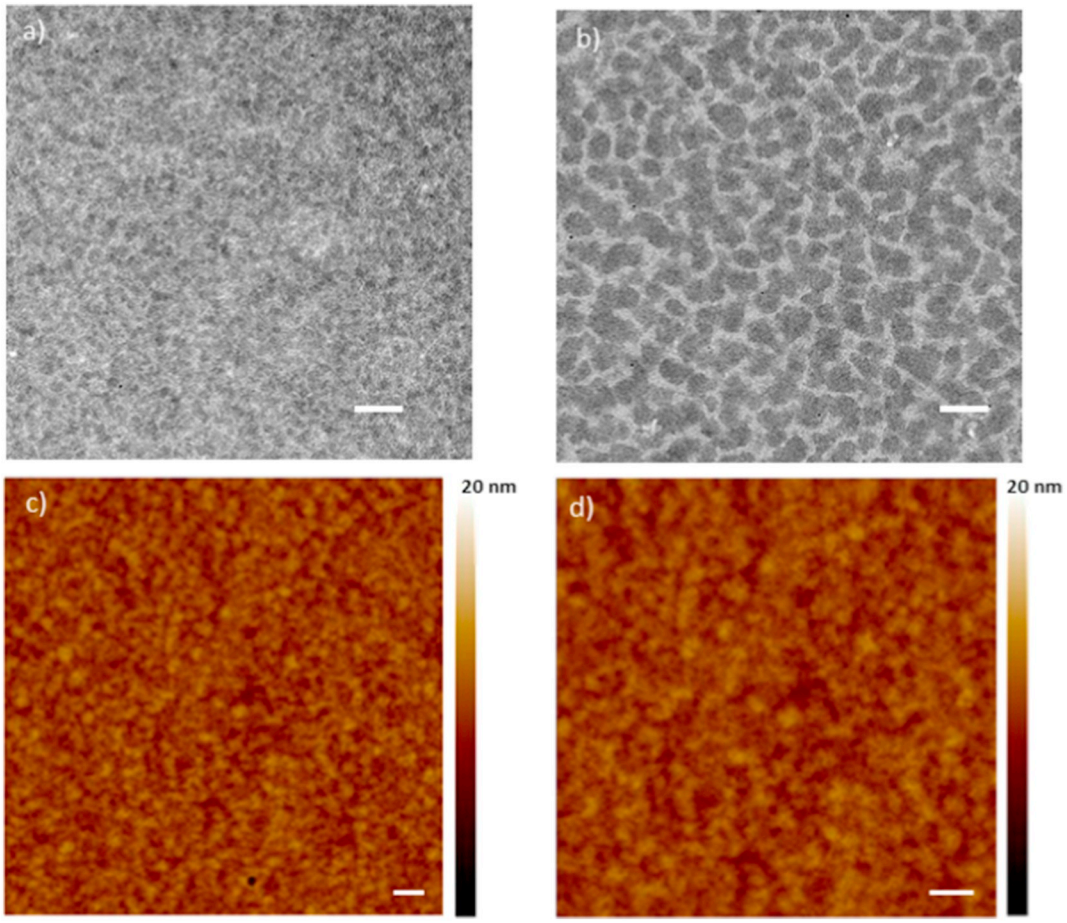

Fig. 7. TEM images of P1:$PC_{71}BM$ (1:3) based active layers processed from (a) *o*-dcb (b) 3% DPE, *o*-dcb and AFM images of P1:$PC_{71}BM$ (1:3) based active layers processed from (c) *o*-dcb (d) 3% DPE, *o*-dcb (scale bar is 200 nm).

were calculated as 1.65 eV and 1.40 eV, respectively. Polymer films showed multi chromic behavior. Under different applied potentials, they exhibited a color range. Table 2illustrates the colorimetric values of the polymer film. L, a, and b values were defined by Commission Internationale de l'Eclairage (ICE). L stands for luminescence, a stands for red/green coordinate and b stands for yellow/blue coordinate.

Optical contrast and switching time of the conjugated polymers were determined via kinetic studies. In order to conduct kinetic studies, 3 mg of the polymers were dissolved in chloroform and spray coated onto ITO coated glass substrate. The polymer films were placed in a cell which contains 0.1 M $TBAPF_6$/ACN electrolyte/solvent system. Neutral and fully oxidized state potentials were applied to the polymers in a certain time interval; 5 s. Potentials were applied at certain wavelengths specified at UV–Vis near IR spectra of the polymers. Investigations of optical contrast and switching time of the polymers were achieved by a square wave potential step technique incorporated with UV–Vis spectrophotometer.

Percent optical contrast values for P1 and P2 were recorded with respect to the specified wavelengths; 445 nm/615 nm and 645 nm, respectively in visible region and percent optical contrast values were recorded at those wavelengths. During the potential switch from oxidation potential to reduction potential in 5 s time interval, UV–Vis spectrophotometer was used to monitor the optical transmittance of the polymers. Kinetic studies of polymers revealed that percent transmittance change for P1 is 20% with a switching time of 1.2 s at 445 nm while showing a 30% with a switching time of 2.0 s at 615 nm and comparatively 11% with a switching time of 1.3 s at 645 nm for P2 (Table 3).

3.2. Organic solar cells studies

In recent years, bulk heterojunction (BHJ) organic solar cells have been the best alternative for device architectures due to the fact that it can efficiently dissociate photogenerated excitons. Since various notions have been developed during the years, BHJ devices require various internal processes. BHJ devices are generally based on blending a conjugated polymer with fullerene derivatives, other conjugated polymers (non-fullerene acceptors) or with inorganic materials to design hybrid solar cells [31,32]. Recently, studies prove that quinoxaline and BDT based conjugated polymers are promising for organic solar cells. Zou and co-workers reported high efficiency organic solar cells up to based on quinoxaline and BDT bearing conjugated polymers [33,34]. Moreover, Zhou and co-workers reported quinoxaline and thiophene containing polymers having PCE values ranging between 8.6% and 13.1% upon introducing fluorine and sulfur atoms into the polymers [35]. In this report, constructed devices are based on blending polymers with fullerene ($PC_{71}BM$). $PC_{71}BM$ was preferred as the acceptor in polymer:acceptor blend to improve the absorption. Polymers were dissolved in *o*-dcb and polymer $PC_{71}BM$ ratio optimizations were carried out. The mixtures were kept in glove box under an inert atmosphere overnight at a certain temperature in order for the polymers to disperse completely in the solvent. The active layer solutions were spin cast as photoactive layers onto the glass substrate coated with ITO and PEDOT:PSS. LiF and Al were deposited on these layers as 0.6 nm and 100 nm, respectively. Resulting device architecture is ITO/PEDOT:PSS/Polymer:$PC_{71}BM$/LiF/Al. In Fig. 5, energy level diagram is represented for the devices.

Photovoltaic devices were constructed with the Polymer:$PC_{71}BM$ ratios of 1:1, 1:2, 1:3 and 1:4. Photovoltaic parameters were summarized in Table 4. 1:1 polymer:$PC_{71}BM$ ratio device showed a power conversion efficiency of 2.22%. Among all the devices based on P1, 1:3 ratio blend demonstrated the best power conversion efficiency of 4.04% with a V_{OC} of 0.67 V, a J_{SC} of 13.94 mA/cm^2, and a FF of 43.3%. *J-V* characteristics of optimized devices are shown in Fig. 6. When the ratio was increased from 1:3 to 1:4 the power conversion efficiency dramatically decreased. Considering that there is a balance between absorbance and charge transport of active layer in organic solar cells, the ratio of acceptor ($PC_{71}BM$) will affect the charge transport. Lower $PC_{71}BM$ ratio in active layer restricts electron transport while high ratios restrict absorbance and hole transport [36]. Therefore, abovementioned decrease in efficiency due to ranging ratio of $PC_{71}BM$ can be attributed to this phenomenon. With the addition of 3% DPE as the solvent additive, a 2.82% PCE value was obtained with the V_{OC} of 0.69 V, a J_{SC} of 8.53 mA/cm^2 and a FF of 48%. Solar cells based on P2 were also fabricated however a PCE value of 0.7% was obtained due to poor film formation.

In order to investigate the active layer morphology and topography, TEM and AFM analyses were performed. Diphenyl ether (DPE) addition usually improves the morphology of the active layer thus raises the PCE values. However, in this study, with the addition of 3% DPE, PCE value decreased to 2.82%. TEM data enable us to rationalize this decrease in PCE. As seen in Fig. 7 (b) with the addition of DPE as the solvent additive, larger domains when compared to the domains in Fig. 7 (a) were formed at a size of 150–200 nm. Domains larger than exciton diffusion length lead to lower J_{SC} values due to reduced charge formation. Similar morphological properties were observed with AFM, AFM images are in good correlation with the TEM images. Active layers processed from *o*-dcb, 3% DPE mixture have very close root mean square values (0.9 nm).

4. Conclusions

Stille polycondensation reaction was applied to synthesize new donor-acceptor type 2D conjugated polymers. BDT was used as the donor unit. Selenophene and furan were used as the π-bridges. The properties of polymers, regarding the effects of selenophene and furan bridging units, on electrochemical, optical and photovoltaic studies were investigated. The polymers have broad absorption and are soluble in common organic solvents. In organic solar cell studies, the best results were obtained with P1. P1:$PC_{71}BM$ with a ratio of 1:3 gave a PCE of 4.04%, a V_{OC} of 0.67 V, a J_{SC} of 13.94 mA/cm^2, and a FF of 43.3%. These results signify that P1 being soluble in common organic solvents is promising for the application in organic solar cells.

Acknowledgments

The authors are grateful to Scientific and Technological Research Council of Turkey (TUBITAK), Grant number: 2210-C, METU-BAP for financial support in this study and to METU Central Laboratory for AFM and TEM analyses.

References

[1] J. Yuang, J. Ouyang, V. Cimrova, M. Leclerc, A. Najari, Y. Zou, Development of quinoxaline based polymers for photovoltaic applications, J. Mater. Chem. C 5 (2017) 1858–1879, https://doi.org/10.1039/C6TC05381E.

[2] R. Wang, R. Ramaraj, T. Okajima, F. Kitamura, N. Matsumoto, T. Thiemann, S. Mataka, T. Ohsaka, Electrochemical behavior of conjugated quinoxaline derivatives, J. Electroanal. Chem. 567 (2004) 85–94, https://doi.org/10.1016/j.jelechem.2003.12.016.

[3] H. He, M. Wang, J. Zhao, Y. Zhang, Poly (10,12-bis(4-hexylthiophen-2-yl)thieno [30,40:5,6]pyrazino[2,3-f] [1,10] – phenanthroline)-coppler(II) complex as an efficient electrocatalyst for oxygen reduction, Chem. Eng. J. 316 (2017) 680–691, https://doi.org/10.1016/j.cej.2017.02.016.

[4] M. Bolognesi, D. Gedefaw, D. Dang, P. Henriksson, W. Zhuang, M. Tessarolo, E. Wang, M. Muccini, M. Seri, M.R. Andersson, 2D π-conjugated benzo[1,2-b:4,5-b'] dithiophene- and quinoxaline-based copolymers for photovoltaic applications, RSC Adv. 3 (2013) 24543–24552, https://doi.org/10.1039/C3RA44238A.

[5] D.A. Gedefaw, Y. Zhou, Z. Ma, Z. Genene, S. Helström, F. Zhang, W. Mammo, O. Inganäs, M.R. Andersson, Conjugated polymers with polar side chains in bulk heterojunction solar cell devices, Polym. Int. 63 (2014) 22–30, https://doi.org/10.1002/pi.4600.

[6] Y. Zhang, J. Zou, H.L. Yip, K.S. Chen, D.F. Zeigler, Y. Sun, A.K.Y. Jen, Indacenodithiophene and quinoxaline-based conjugated polymers for highly efficient polymer solar cells, Chem. Mater. 23 (2011) 2289–2291, https://doi.org/10.1021/cm200316s.

[7] Y. Zhang, L. Kong, H. Du, J. Zhao, Y. Xie, Three novel donor-acceptor type electrochromic polymers containing 2,3-bis(5-methylfuran-2-yl)thieno[3,4-b]pyrazine acceptor and different thiophene donors: low-band-gap, neutral green-colored, fast-switching materials, J. Electroanal. Chem. 830-831 (2018) 7–12, https://doi.org/10.1016/j.jelechem.2018.10.020.

[8] W. Su, M. Xiao, Q. Fan, J. Zhong, J. Chen, D. Dang, J. Shi, W. Xiong, X. Duan, H. Tan, Y. Liu, W. Zhu, Significantly increasing open-circuit voltage of the benzo [1,2-b:4,5-b']dithiophene-alt-5,8-dithienyl-quinoxaline copolymers based PSCs by appending dioctyloxy chains at 6,7-positions of quinoxaline, Org. Electron. 17 (2015) 129–137, https://doi.org/10.1016/j.orgel.2014.11.021.

[9] J. Yuan, L. Qiu, Z.G. Zhang, Y. Li, Y. Chen, Y. Zou, Tetrafluoroquinoxaline based polymers for non-fullerene polymer solar cells with efficiency over 9%, Nano Energy 30 (2016) 312–320, https://doi.org/10.1016/j.nanoen.2016.10.008.

[10] M.L. Keshtov, D.Y. Godovsky, S.A. Kuklin, A. Nicolaev, J. Lee, B. Lim, H.K. Lee, E.N. Koukaras, G.D. Sharma, Synthesis and photophysical properties of semiconductor molecules D1-A-D2-A-D1-type structure based on derivatives of quinoxaline and dithienosilole for organics solar cells, Org. Electron. 39 (2016) 361–370, https://doi.org/10.1016/j.orgel.2016.10.010.

[11] W.H. Tseng, H.C. Chen, Y.C. Chien, C.C. Liu, Y.K. Peng, Y.S. Wu, J.H. Chang, S.H. Liu, S.W. Chou, C.-L. Liu, Y.H. Chen, C.I. Wu, P.T. Chou, Comprehensive study of medium-band gap conjugated polymer merging a fluorinated quinoxaline with branched side chains for highly efficient and air-stable polymer solar cells, J. Mater. Chem. A 2 (2014) 20203–20212, https://doi.org/10.1039/C4TA05062B.

[12] Z. Fei, R.S. Ashraf, Y. Han, S. Wang, C.P. Yau, P.S. Tuladhar, T.D. Anthopoulos, M.L. Chabinyc, M. Heeney, Diselenogermole as a novel donor monomer for low band gap polymers, J. Mater. Chem. A 3 (2015) 1986–1994, https://doi.org/10.1039/C4TA05703A.

[13] Z. Fei, Y. Han, E. Gann, T. Hodsden, A.S.R. Chesman, C.R. McNeill, T.D. Anthopoulos, M. Heeney, Alkylated selenophene-based ladder-type monomers via a facile route for high-performance thin-film transistor applications, J. Am. Chem. Soc. 139 (25) (2017) 8552–8561, https://doi.org/10.1021/jacs.7b03099.

[14] Y. Hwang, G. Ren, N.M. Murari, S.A. Jenekhe, n-type naphthalene diimide–biselenophene copolymer for all-polymer bulk heterojunction solar cells, Macromolecules 45 (2012) 9056–9062, https://doi.org/10.1021/ma3020239.

[15] M.J. Sung, A. Luzio, W.T. Park, R. Kim, E. Gann, F. Maddalena, G. Pace, Y. Xu, D. Natali, C. de Falco, L. Dang, C.R. McNeill, M. Caironi, Y.Y. Noh, H. Kim, High mobility naphthalene diimide and selenophene vinylene selenophene based conjugated polymer: n-channel organic field effect transistors and structure–property relationship, Adv. Funct. Mater. 26 (2016) 4984–4997, https://doi.org/10.1002/adfm.201601144.

[16] E.H. Jung, S. Bae, T.W. Yoo, W.H. Jo, The effect of different chalcogenophenes in isoindigo-based conjugated copolymers on photovoltaic properties, Polym. Chem. 5 (2014) 6545–6550, https://doi.org/10.1039/C4PY00791C.

[17] S. Goker, G. Hizalan, M. Ileri, S.O. Hacioglu, L. Toppare, The effect of the different donor units on fluorescent conjugated polymers containing 2,1,3-benzooxadiazole as the acceptor unit, J. Electroanal. Chem. 751 (2015) 80–89, https://doi.org/10.1016/j.jelechem.2015.05.028.

[18] A.T. Yiu, P.M. Beaujuge, O.P. Lee, C.H. Woo, M.F. Toney, J.M.J. Frechet, Side-chain tunability of furan-containing low-band-gap polymers provides control of structural order in efficient solar cells, J. Am. Chem. Soc. 134 (4) (2012) 2180–2185, https://doi.org/10.1021/ja2089662.

[19] C.H. Woo, P.M. Beaujuge, T.W. Holcombe, O.P. Lee, J.M.J. Frechet, Incorporation of furan into low band-gap polymers for efficient solar cells, J. Am. Chem. Soc. 132 (44) (2010) 15547–15549, https://doi.org/10.1021/ja108115y.

[20] P.A. Peart, J.D. Tovar, Expanding the realm of furan-based conducting polymers through conjugation with 1,6-Methano[10]annulene, Macromolecules 42 (2009) 4449–4455, https://doi.org/10.1021/ma9006494.

[21] R.C. Coffin, J. Peet, J. Rogers, G.C. Bazan, Streamlined microwave-assisted preparation of narrow-bandgap conjugated polymers for high-performance bulk heterojunction solar cells, Nat. Chem. 1 (2009) 657–661, https://doi.org/10.1038/nchem.403.

[22] W. Li, W.S.C. Roelofs, M.M. Wienk, R.A.J. Janssen, Enhancing the photocurrent in diketopyrrolopyrrole-based polymer solar cells via energy level control, J. Am. Chem. Soc. 134 (33) (2012) 13787–13795, https://doi.org/10.1021/ja305358z.

[23] a) Y. Wang, Y. Liu, S. Chen, R. Peng, Z. Ge, Significant enhancement of polymer solar cell performance via side-chain engineering and simple solvent treatment, Chem. Mater. 25 (15) (2013) 3196–3204, https://doi.org/10.1021/cm401618h; b) X. Wang, S. Chen, Y. Sun, M. Zhang, Y. Li, X. Li, H. Wang, A furan-bridged D-π-A copolymer with deep HOMO level: synthesis and application in polymer solar cells, Polym. Chem. 2 (2011) 2872–2877, https://doi.org/10.1039/C1PY00364J.

[24] H. Pan, Y. Li, Y. Wu, P. Liu, B.S. Ong, S. Zhu, G. Xu, Low-temperature, solution-processed, high-mobility polymer semiconductors for thin-film transistors, J. Am. Chem. Soc. 129 (14) (2007) 4112–4113, https://doi.org/10.1021/ja067879o.

[25] L. Hou, J. Hou, S. Zhang, H.-Y. Chen, Y. Yang, A polybenzo[1,2-b:4,5-b']dithiophene derivative with deep HOMO level and its application in high performance

polymer solar cells, Angew. Chem. Int. Ed. 49 (2011) 1500–1503, https://doi.org/10.1002/ange.200906934.
[26] Y. Zhang, L. Gao, C. He, Q. Sun, Y. Li, Synthesis and photovoltaic properties of two-dimension-conjugated D–A copolymers based on benzodithiophene or benzodifuran units, Polym. Chem. 4 (2013) 1474–1481, https://doi.org/10.1039/C2PY20910A.
[27] L. Dou, J. Gao, E. Richard, J. You, C.C. Chen, K.C. Cha, Y. He, G. Li, Y. Yang, Systematic investigation of benzodithiophene- and diketopyrrolopyrrole-based low-bandgap polymers designed for single junction and tandem polymer solar cells, J. Am. Chem. Soc. 134 (24) (2012) 10071–10079, https://doi.org/10.1021/ja301460s.
[28] L. Hou, S. Zhang, X. Guo, F. Xu, Y. Li, J.H. Hou, Replacing alkoxy groups with alkylthienyl groups: a feasible approach to improve the properties of photovoltaic polymers, Angew. Chem. Int. Ed. 50 (2011) 9697–9702, https://doi.org/10.1002/ange.201103313.
[29] M. Zhang, Y. Gu, X. Guo, F. Liu, S. Zhang, L. Huo, T.P. Russell, J.H. Hou, Efficient polymer solar cells based on benzothiadiazole and alkylphenyl substituted benzodithiophene with a power conversion efficiency over 8%, Adv. Mater. 25 (2013) 4944–4949, https://doi.org/10.1002/adma.201301494.
[30] R. Duan, L. Ye, X. Guo, Y. Huang, P. Wang, S. Zhang, J. Zhang, L. Huo, J. Hou, Application of two-dimensional conjugated benzo[1,2-b:4,5-b']dithiophene in quinoxaline-based photovoltaic polymers, Macromolecules 45 (7) (2012) 3032–3038, https://doi.org/10.1021/ma300060z.
[31] G. Dennler, M.C. Scharber, J. Brabec, Polymer-fullerene bulk-heterojunction solar cells, Adv. Mater. 21 (2009) 1323–1338, https://doi.org/10.1002/adma.200801283.
[32] S. Rafique, S.M. Abdullah, K. Sulaiman, M. Iwamoto, Fundamentals of bulk heterojunction organic solar cells: an overview of stability/degradation issues and strategies for improvement, Renew. Sust. Energ. Rev. 84 (2018) 43–53, https://doi.org/10.1016/j.rser.2017.12.008.
[33] J. Yuan, Y. Zhang, L. Zhou, G. Zhang, H.L. Yip, T.K. Lau, X. Lu, C. Zhu, H. Peng, P.A. Johnson, M. Leclerc, Y. Cao, J. Ulanski, Y. Li, Y. Zou, Single-junction organic solar cell with over 15% efficiency using fused-ring acceptor with electron-deficient core, Joule 3 (4) (2019) 1140–1151, https://doi.org/10.1016/j.joule.2019.01.004.
[34] J. Yuan, Y. Zhang, L. Zhou, C. Zhang, T.K. Lau, G. Zhang, X. Lu, H.L. Yip, S.K. So, S. Beaupré, M. Mainville, P.A. Johnson, M. Leclerc, H. Chen, H. Peng, Y. Li, Y. Zou, Fused benzothiadiazole: a building block for n-type organic acceptor to achieve high-performance organic solar cells, Adv. Mater. 31 (2019) 1807577 (1–8, https://doi.org/10.1002/adma.201807577.
[35] J. Yang, P. Cong, L. Chen, X. Wang, J. Li, A. Tang, B. Zhang, Y. Geng, E. Zhou, Introducing fluorine and sulfur atoms into quinoxaline-based p type polymers to gradually improve the performance of fullerene-free organic solar cells, ACS Macro Lett. 8 (2019) 743–748, https://doi.org/10.1021/acsmacrolett.9b00368.
[36] Y. Yang, J. Zhang, Y. Zhou, G. Zhao, C. He, Y. Li, M. Andersson, O. Inganas, F. Zhang, Solution-processable organic molecule with triphenylamine core and two benzothiadiazole-thiophene arms for photovoltaic application, J. Phys. Chem. C 114 (2010) 3701–3706, https://doi.org/10.1021/jp910836t.